In vivo imaging of T cell delivery to tumors after adoptive transfer therapy

Mikael J. Pittet*†‡, Jan Grimm†§, Cedric R. Berger†, Takahiko Tamura†, Gregory Wojtkiewicz†, Matthias Nahrendorf†, Pedro Romero¶, Filip K. Swirski†, and Ralph Weissleder*†

*Center for Systems Biology, Massachusetts General Hospital and Harvard Medical School, Simches Research Building, 185 Cambridge Street, Boston, MA 02114; †Center for Molecular Imaging Research, Massachusetts General Hospital, Harvard Medical School, Charlestown, MA 02129; and ¶Division of Clinical Onco-Immunology, Ludwig Institute for Cancer Research, University Hospital, 1011 Lausanne, Switzerland

Communicated by Diane Mathis, Harvard Medical School, Boston, MA, June 13, 2007 (received for review May 8, 2007)

Adoptive transfer therapy of *in vitro*-expanded tumor-specific cytolytic T lymphocytes (CTLs) can mediate objective cancer regression in patients. Yet, technical limitations hamper precise monitoring of posttherapy T cell responses. Here we show in a mouse model that fused single photon emission computed tomography and x-ray computed tomography allows quantitative whole-body imaging of ^{111}In-oxine-labeled CTLs at tumor sites. Assessment of CTL localization is rapid, noninvasive, three-dimensional, and can be repeated for longitudinal analyses. We compared the effects of lymphodepletion before adoptive transfer on CTL recruitment and report that combined treatment increased intratumoral delivery of CTLs and improved antitumor efficacy. Because ^{111}In-oxine is a Food and Drug Administration-approved clinical agent, and human SPECT-CT systems are available, this approach should be clinically translatable, insofar as it may assess the efficacy of immunization procedures in individual patients and lead to development of more effective therapies.

cancer | immunity | CD8 T cell

Leukocytes play a critical role in cancer. Studies in both patients and animal models have shown that T cells infiltrate tumor stroma and recognize antigenic peptides expressed by tumor cells (1–4). Tumor-specific CD8 cytolytic T lymphocytes (CTLs) derived from cancer patients recognize and kill tumors *in vitro*, yet the same cells often fail to eradicate cancer *in vivo* (5), likely because of endogenous mechanisms of suppression (6, 7). Among these, regulatory T cells have emerged as central constituents of suppressive activity, because they efficiently infiltrate tumor stroma (8–10), interfere with tumor-specific CTL cytolytic activity (11, 12), and reduce survival (13, 14). To break such dominant tolerance mechanisms, at least two types of immunotherapeutic strategies are being pursued currently: (*i*) *in vivo* activation of endogenous antitumor cells (1) and (*ii*) adoptive transfer of *in vitro*-activated antitumor cells (15, 16). In clinical trials based on the latter, tumor antigen-specific T cells are isolated from the patient, induced to expand to high numbers *in vitro*, and reinjected (17, 18). This strategy generates a large pool of functional CTLs that can kill tumor cells *in vivo*. In a further modification of this approach, the patient is lymphodepleted before adoptive transfer, a procedure that eliminates endogenous suppressor cells and favors *in vivo* expansion and persistence of the transferred CTLs (19, 20). This approach appears to be effective for treatment of melanoma patients, because it leads to objective tumor regression in >50% of patients (21).

Assessing the efficacy of immunotherapeutic approaches in patients requires noninvasive and sensitive cell-tracking technologies. Current methods quantify transferred cells either in peripheral blood or in fine-needle tumor aspirates; whereas the former cannot colocalize CTLs with the tumor, the latter is invasive, impractical, and prone to sampling bias. Recent advances in optical, magnetic resonance, and nuclear imaging technologies (22–24), however, permit noninvasive and longitudinal cell tracking in their native environment. High-resolution small animal imaging systems are now in widespread use, but not all are suitable for clinical translation today. In optical imaging, for instance, transgenes such as fluorescent proteins and luciferases are potentially immunogenic and favor surface-weighted signals (24–26). Other agents such as HSV-Tk for nuclear positron emission tomography imaging (23) also have reported immunogenicity (27). Finally, cell trackers for magnetic resonance imaging are not yet Food and Drug Administration (FDA)-approved and do not permit tracking in all tissues. Single-photon emission computed tomography (CT)–x-ray CT (SPECT-CT) fusion imaging, however, offers many advantages that favor its use as clinical reporter of cell migration in cancer immunotherapy. High-sensitivity gammacameras detect high-energy photons emitted from cell trackers, whereas x-ray scanners provide information on tissue density; the inclusion of both scanners in the same imaging system allows whole-body 3D anatomic localization of labeled cells with exceptional sensitivity and resolution. Second, the cell tracker ^{111}Indium-oxine is biocompatible, nonimmunogenic, inexpensive, simple to use, FDA-approved, and has a relatively long half-life (2.8 days) (28). Given these attributes, we conducted the current study to validate this imaging approach and compare results of accepted gold standards used in the field. We show in a model system of adoptive transfer immunotherapy that SPECT-CT combines precise tracking of administered CTLs and allows monitoring of tumor growth or rejection *in vivo*.

Results

Antigen-Specific CTLs Kill Tumors *in Vitro* and Control Tumor Growth *in Vivo*. To establish a model of adoptive transfer immunotherapy, we injected 10^6 CT44 tumor cells into the right footpad and 10^6 CT26 tumor cells into the left footpad of Thy1.1 BALB/c mice (day 0, Fig. 1*A*). As described (11, 12), these two cell lines differ in that CT44 tumor cells express HA. Both tumors grew rapidly and had reached a size of ≈25 mm^2 after 7 days. In parallel, we expanded HA-specific CTLs *in vitro*. We obtained these cells from *TCR-CL4 RAG*$^{-/-}$ Thy1.2 BALB/c mice that express a transgenic TCR specific for the K_d-restricted $HA_{512–520}$ peptide (12). When stimulated *in vitro* with cognate peptide and IL-2, HA-specific CTLs killed HA$^+$ CT44 tumor cells efficiently and selectively in ^{51}Cr-release

Author contributions: M.J.P., J.G., and C.R.B. contributed equally to this work; M.J.P., J.G., P.R., F.K.S., and R.W. designed research; M.J.P., J.G., C.R.B., T.T., G.W., and F.K.S. performed research; P.R. and R.W. contributed new reagents/analytic tools; M.J.P., J.G., C.R.B., T.T., G.W., M.N., F.K.S., and R.W. analyzed data; and M.J.P., J.G., C.R.B., F.K.S., and R.W. wrote the paper.

The authors declare no conflict of interest.

Abbreviations: CTL, cytolytic T lymphocyte; CT, computed tomography; SPECT-CT, single-photon emission CT–x-ray CT; ROI, region of interest; PI, postinjection.

‡To whom correspondence should be addressed. E-mail: mpittet@mgh.harvard.edu.

§Present address: Memorial Sloan–Kettering Cancer Center, Department of Radiology, New York, NY 10044.

This article contains supporting information online at www.pnas.org/cgi/content/full/0704460104/DC1.

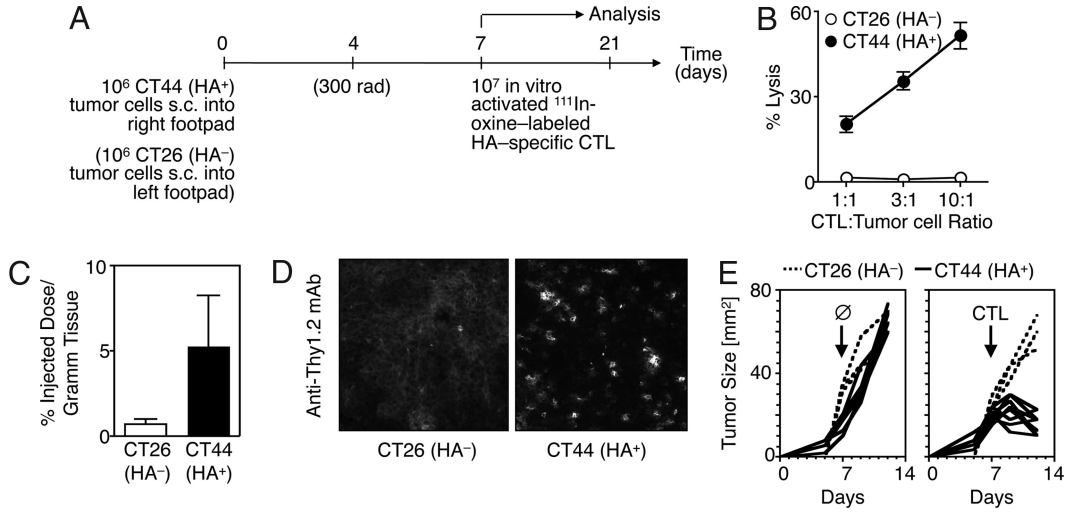

Fig. 1. Antigen-specific CTL-mediated antitumor response. (*A*) Outline of the experimental design. (*B*) *In vitro*-stimulated HA-specific CTLs specifically lyse CT44 HA$^+$ tumor cells in ^{51}Cr-release assays. (*C*) ^{111}In-Oxine-labeled HA-specific CTLs selectively accumulate in HA$^+$ tumors, as determined by calculating the percentage of ^{111}in-injected dose/gram tissue in explanted tumors 96 h after adoptive T cell transfer. (*D*) Thy1.2$^+$ HA-specific CTLs selectively accumulate in HA$^+$ tumors implanted in Thy1.1$^+$ animals, as determined by immunohistochemical analysis of tumor parenchyma. (*E*) Administered HA-specific CTLs selectively control HA$^+$ CT44 tumor growth; n = 3–10.

assays (Fig. 1*B*). To assess their capacity to control tumor growth *in vivo*, 10^7 HA-specific CTLs were labeled with ^{111}In-oxine, a cell tracker that does not elicit any major changes in cell function at diagnostic doses [data not shown and (29)]. Labeled cells were injected intravenously into mice that had received tumor cells 7 days earlier (Fig. 1*A*). HA-specific CTLs accumulated preferentially in HA$^+$ tumors *in vivo*, as identified in biodistribution assays on explanted tumors (Fig. 1*C*) and by immunohistochemistry on tumor sections (Fig. 1*D*). As expected, the CTLs selectively controlled progression of HA$^+$ tumors (Fig. 1*E*). This experimental system, therefore, offered the possibility to use SPECT-CT to assess whether this platform may allow *in vivo* noninvasive monitoring of CTL delivery to the tumor site.

SPECT-CT for *in Vivo* Tracking of Adoptively Transferred Cells. Mice bearing HA$^+$ CT44 and HA$^-$ CT26 tumors for 7 days in the right and left footpad, respectively, received 10^7 ^{111}In-labeled HA-specific CTLs intravenously and were subjected to SPECT-CT periodically [2, 24, 48, and 120 h postinjection (PI)]. The vast majority of ^{111}In–labeled HA-specific CTLs accumulated in the lungs 2 h PI but rapidly redistributed to the liver and spleen within 24 h [Fig. 2*A* and supporting information (SI) Movies 1 and 2]. As early as 2 h after transfer, CTL accumulated in the tumors and increased in HA$^+$ CT44 tumors by 24 h compared with controls (Fig. 2 *B* and *C*). The CTLs accumulated preferentially and in increasing concentrations in CT44 tumors for the duration of the experiment, whereas the concentration of CTLs in CT26 tumors remained unchanged (Fig. 2 *B–D* and SI Movies 3 and 4). We also observed a different pattern of signal distribution in the tumors. Specifically, in the CT44 tumors the signal localized centrally, whereas in the CT26 tumors, it was diffuse and marginalized. This suggests that the HA-specific CTLs accumulated throughout the HA-expressing tumors but remained at the periphery of the HA$^-$ tumors. These findings confirm observations by intravital microscopy that deep infiltration of CTLs to the tumor bulk requires expression of tumor-specific cognate antigen (30, 31). The inclusion of x-ray CT in the SPECT-CT system allowed us to evaluate not only the anatomical location of the tumor but also evolution of tumors. Hence, we could evaluate the effect of immunotherapy by correlating *in vivo* localization of CTLs, as determined by SPECT, with tumor size, as determined by x-ray CT. We observed that HA-specific CTLs controlled HA$^+$ CT44 but not HA$^-$ CT26 tumor growth (Fig. 2*E*). In control experiments, we used syngeneic CTLs specific for an irrelevant antigen (tERK-I) and confirmed that these CTLs failed to accumulate and control growth of either HA$^+$ CT44 or HA$^-$ CT26 tumors (SI Fig. 4 and data not shown).

Lymphopenia Promotes CTL Recruitment and Control of Tumor Growth. Studies have shown that lymphodepletion augments antitumor T cell efficacy in humans (19, 21, 32) and in animals (33–35). We therefore sought to investigate *in vivo* with SPECT-CT whether lymphopenia controls tumor growth through effects on CTL accumulation. Mice received 10^6 CT44 tumor cells in the right footpad, were lymphodepleted (300 rad irradiation that depletes nearly all circulating lymphocytes) on day 4, and injected with HA-specific CTLs on day 7. Lymphodepletion alone led to slight reduction of tumor growth at least between days 7 and 12, although tumor size at later time points (e.g., day 14) was comparable in mice that received no treatment or irradiation alone (Fig. 3*A*). This effect was likely mediated by "homeostatic proliferation" of endogenous immune cells that can exhibit antitumor activity (33). It has also been demonstrated previously that irradiation, at the doses used here, of the tumor alone fails to elicit regression, and shielding the tumor from irradiation does not decrease antitumor efficacy in the adoptive T cell transfer setting (34). CTL injection alone led to control of tumor growth, as described above. Combined lymphodepletion and CTL therapy, however, led to most efficient control of tumor growth (Fig. 3*A*). SPECT-CT imaging demonstrated that control of tumor growth associated with increased density of CTLs at the tumor site (Fig. 3 *B* and *C*). Flow cytometry confirmed that CTLs preferentially accumulated in lymphodepleted animals (Fig. 3*D*). These data show that lymphopenia promotes antitumor function partly via effects on CTL accumulation at tumor sites.

Discussion

This study shows that SPECT-CT is effective for simultaneously tracking migration of administered CTLs to tumors and monitoring tumor volume *in vivo*. Accumulation and continued

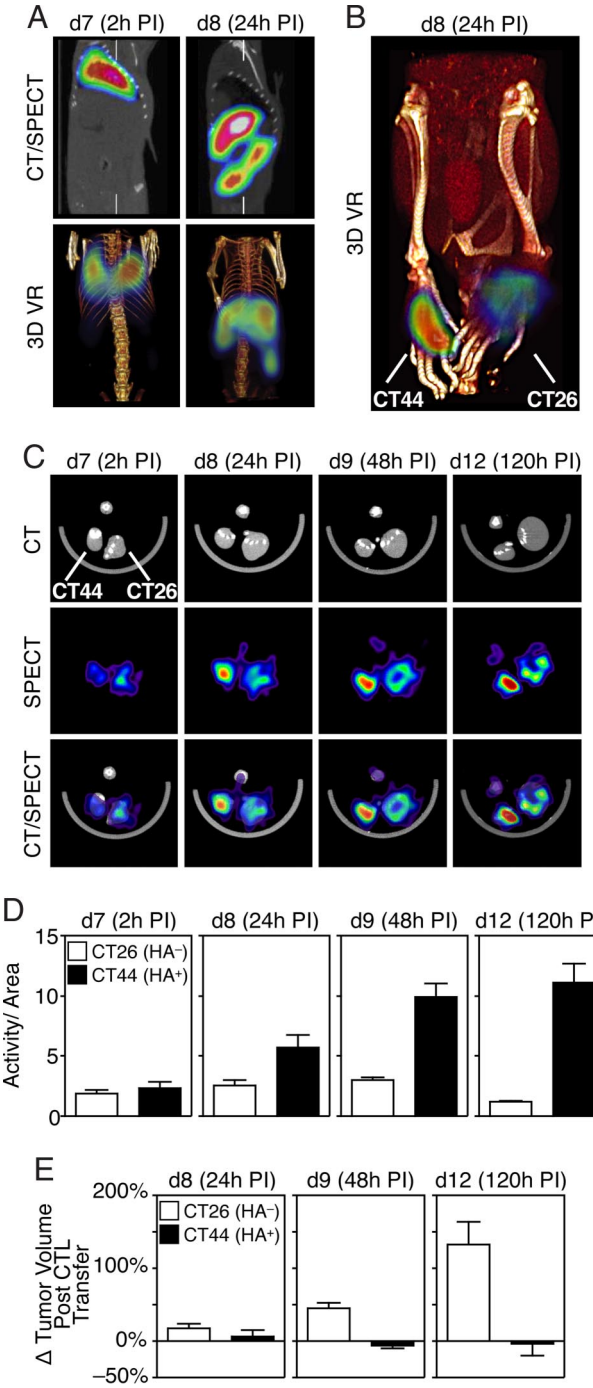

Fig. 2. *In vivo* SPECT-CT monitoring of CTL distribution after adoptive transfer. (*A*) Fused SPECT-CT scans (*Upper*) and 3D virtual rendering (3D VR) images of anesthetized mice obtained 2 h (*Left*) and 24 h (*Right*) PI of ^{111}In-labeled HA-specific CTLs. Mice received CT44 HA$^+$ and CT26 HA$^-$ tumor cells in the right and left footpads, respectively, on day 0, and the CTLs on day 7 (the mice did not receive irradiation). The CTLs accumulated in the lung 2-h PI and in the liver and spleen 24 h PI (see also SI Movies 1 and 2). (*B*) 3D VR view of HA-specific CTL accumulation in HA$^+$ and HA$^-$ tumors (see also SI Movie 3). (*C*) CT, SPECT, and SPECT-CT fusion images obtained 2, 24, 48, and 120 h PI show specific accumulation of HA-specific CTLs in HA$^+$ tumors. (*D*) Ratios of SPECT activity to ROI area calculated 2, 24, 48, and 120 h PI indicate specific accumulation of HA-specific CTLs in HA$^+$ tumors. (*E*) Tumor volumes calculated by x-ray CT indicate that administered HA-specific CTLs control HA$^+$ CT44 tumor growth. Data shown indicate changes (Δ) in HA$^+$ CT44 and HA$^-$ CT26 tumor volumes at the indicated time points when compared with tumor volumes at the time of CTL transfer [i.e., day 7 (d7)]; n = 5–10.

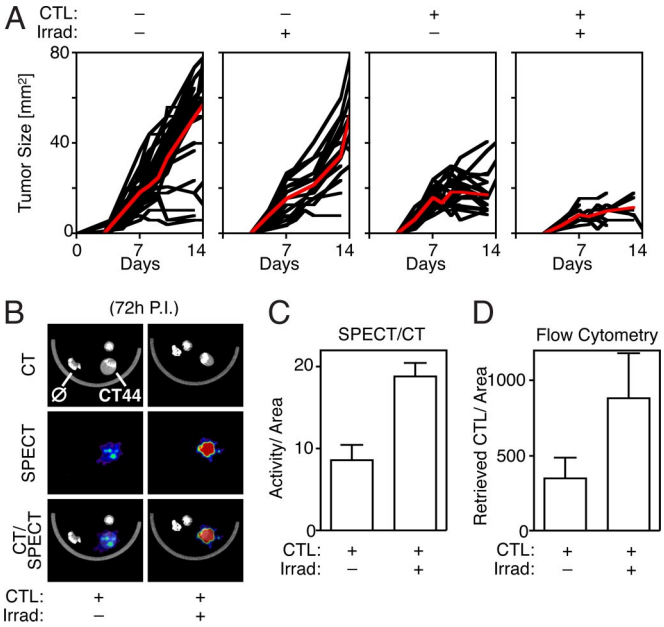

Fig. 3. *In vivo* SPECT-CT monitoring for comparison of immunotherapeutic strategies. (*A*) CT44 HA$^+$ tumor growth kinetics in mice treated with HA-specific CTLs (administered on day 7) and lymphodepleted (irradiated on day 4), either alone or in combination. Red lines indicate mean values for all mice analyzed; n = 12–30. (*B*) CT, SPECT, and SPECT-CT fusion images obtained 72 h PI show increased ^{111}in-CTL activity in tumors of lymphopenic mice. (*C*) Quantification of SPECT-CT data reveals increased ^{111}in-CTL activity 72 h PI in tumors of lymphopenic mice; n = 3. (*D*) Flow cytometric analysis of HA-specific CTL accumulation in HA$^+$ tumors 72 h PI confirms the SPECT-CT findings; n = 3.

presence of administered CTLs at the tumor site is antigen-dependent and intratumoral CTL accumulation and tumor regression improves when CTLs are injected to lymphopenic hosts. This longitudinal, quantitative, and *in vivo* study in experimental cancer immunotherapy reveals a dynamic interplay between tumor progression and CTL accumulation. We therefore propose that immunotherapeutic strategies harness the unique advantages offered by SPECT-CT for longitudinal monitoring of transferred cells in single patients.

Although adoptive transfer therapy shows great promise at controlling tumor growth and indeed has proven efficacious in several clinical trials for melanoma patients, the strategy requires fine-tuning and broader applicability. Several experimental and preclinical studies have shown that lymphodepletion in melanoma patients before CTL transfer improves antitumor efficacy, thus encouraging the widespread use of this procedure in the clinic (21). Moreover, adoptive transfer of donor lymphocytes or allogeneic hematopoietic stem cells is actively explored in a number of therapeutic applications for the control and/or prevention of viral infections (36), generation of selective graft vs. leukemia effects (37, 38), and treatment of autoimmunity (39, 40). Using SPECT-CT, we demonstrate that lymphopenia fosters tumor rejection partly because it promotes efficient CTL accumulation at the tumor site. It will be important to determine why similar treatments are ineffective at controlling cancers other than melanomas. A number of immunotherapeutic strategies are currently under investigation. For instance, adoptive transfer of less-differentiated T cells appears considerably more potent at protecting hosts with advanced tumors (41). This can be achieved by culturing *in vitro* antigen-primed CD8 T cells with IL-15 (42) or IL-21 (43). These cells resemble central memory cells and show proliferative potential and migration to lymph nodes *in vivo* (41). Lymph node homing or *in vivo* expansion, these findings suggests, may be essential for long-term control of tumor growth.

Another set of studies suggests that tumor rejection can be achieved by altering the intratumoral balance of CTLs and regulatory T cells (44). Finally, use of chimeric T cell receptors shows promise for improving therapy (20). The need to assess the efficacy of various adoptive transfer therapies, as highlighted by these examples, underscores the need for techniques such as SPECT-CT to reliably monitor cell migration *in vivo*.

This study exemplifies the capacity of SPECT-CT to enable noninvasive and longitudinal imaging of ^{111}In-oxine-labeled CTLs, and newly identifies that lymphopenic conditions increase the delivery of CTLs at tumor sites. In the future, it will be important to use genetically engineered mouse models of spontaneous rather than transplantable cancer (45), because they may better translate retrieved information into humans with cancer. The methods described in this study also have immediate clinical applicability: clinical scanners are available, and ^{111}In-oxine has been used in patients for several decades to track leukocytes by planar scintigraphy (46). We hope this study will serve to accelerate efforts to monitor administered cells for *in vivo* evaluation of immune responses in single patients. Because SPECT-CT offers the unique possibility of tracking two different populations simultaneously (47), future studies may elect to monitor the interplay between different cell types that may display antitumor efficacy (e.g., subsets of CD8 and CD4 T cells, NK cells) and thus show promise as cell-based clinical immunotherapies. In addition, the approach described here will likely continue to be useful for assessing efficacy of immunization procedures experimentally.

Methods

Mice. TCR-CL4 RAG$^{-/-}$ BALB/c mice expressing a TCR specific for $K^d/HA_{512–520}$ were generated as described (11). DUC18 BALB/c mice expressing a TCR specific for K^d/tERK-$I_{136–144}$ (48) and Thy1.1 BALB/c mice were obtained from Paul Allen. BALB/c mice were purchased from Taconic (Germantown, NY).

Tumors. The CT26 tumor cell line was derived from a chemically induced murine colon carcinoma. The tumor cell line CT44 was generated by transfecting CT26 cells with a fusion protein of influenza hemagglutinin and EGFP (11). Anesthetized animals received 10^6 CT26 and CT44 cells in 50 μl of PBS s.c. into the upper side of the left and the right hindpaw, respectively.

T Cells. Single-cell suspensions pooled from mesenteric and popliteal lymph nodes and spleen of *TCR-CL4* RAG$^{-/-}$ BALB/c mice were stimulated *in vitro* in complete medium (500 ml of RPMI medium 1640 with sodium 1 mM pyruvate/10 mM Hepes/2 mM glutamin/1% penicilin/streptomycin/50 μM mercaptoethanol/10% FCS previously heat-inactivated for 1 h at 56°C) with 1 μg/ml $HA_{512–520}$ peptide for 1 h, washed, and maintained at 37°C. Starting on day 2 and every second day, cells were harvested and incubated in fresh complete medium supplemented with 20 ng/ml rhIL-2 (R&D Systems, Minneapolis, MN) until day 7. Stimulation of DUC18 T cells involved stimulation with the tERK-I136-144 peptide.

^{111}In-Oxine Labeling. On day 7, *in vitro* expanded HA-specific CTLs (or tERK-I-specific CTLs) were labeled with ^{111}In-Oxine according to the manufacturer's protocol (Amersham Pharmacia Health Medi-Physics, Arlington Heights, IL). Briefly, cells were washed in HBSS and resuspended in ^{111}In-oxine for 20 min at 37°C, pH 6.5–7.5. Cells were washed three times in HBSS and injected into the mice. The total amount of activity injected into each animal was measured with a radioisotope calibrator (Capintec, Ramsey, NJ) immediately PI and before each of the imaging time points to account for differences in activity. As described (28, 29), ^{111}In-oxine does not affect lymphocyte viability or functionality and is fully biocompatible.

SPECT-CT Imaging, Processing, and Analysis Protocol. Serial SPECT-CT projections from anesthetized mice were acquired on a X-SPECT imaging system (Gamma Medica, Northridge, CA) at 2, 24, 48, 72, 96, and 120 h after T cell adoptive transfer. Two imaging sessions were acquired to obtain whole-body imaging of the abdomen and tumor-bearing hindpaws. Photons from the tracer were collimated with a 1-mm pinhole collimator on each camera, resulting in submillimeter resolution. SPECT (radius of rotation 3 cm, 32 projections, 30–120 s per projection) and CT scans (256 projections, 50 kv, 500 mA) were acquired and coregistered for image fusion and exact 3D anatomical localization of the tracer signal. Acquired SPECT and CT data sets were processed with Osirix DICOM viewer software (http://homepage.mac.com/rossetantoine/osirix). Fused SPECT-CT images were examined visually in the transaxial, sagittal, and coronal planes for ^{111}In-Oxine localization in various organs and biodistribution. Mean pixel intensity and tumor volume were determined by designing region of interest (ROIs) in the hindpaws. ROIs were chosen to fit exactly to the organ shape (CT scans) to minimize partial volume errors. The same ROIs were used on SPECT images to assess ^{111}In-Oxine signal. Emission data for each imaging sessions were normalized for counts per projection, imaging time, and ^{111}In-Oxine radioactivity decay. Additionally, after the last scan, some mice were killed for conventional biodistribution analysis.

Flow Cytometry. Tumors were homogenized in a potter (Fisher Scientific, Pittsburgh, PA), further digested with 0.2 mg/ml collagenase IV and 0.04 mg/ml DNase I (Boheringer Mannheim/Roche, Mannheim, Germany) for 30 min at 37°C with gentle agitation, and filtered. Single-cell suspensions were labeled with anti-CD8-FITC and anti-Thy1.2-PE mAb. Data were acquired on a FACScalibur (Becton Dickinson, Franklin Lakes, NJ) and analyzed with FlowJo software (Tree Star, Inc., Ashland, OR).

Immunohistochemistry (IHC). Frozen 8-mm tumor sections were acetone-fixed and incubated with rat anti-Thy1.2 mAb (Becton Dickinson) and further reacted with anti-rat IgG-biotin (Becton Dickinson) and streptavidin-Alexa546 (Molecular Probes). The fluorescence images were generated with a digital-imaging microscope (Nikon, Melville, NY; 80i). Controls included labeling without rat anti-Thy1.2 primary mAb.

We thank Andita Newtown and Peter Waterman for support in performing some experiments. We thank Dr. Paul Allen (Department of Pathology and Immunology, Washington University School of Medicine, St. Louis, MO) for providing Thy1.1 and DUC18 BALB/c mice, Dr. Jose Figueiredo for performing mouse surgeries, Dr. Hanwen Zhang for assistance with cell labeling, and Melissa Carlson for secretarial assistance (Center for Molecular Imaging Research, Massachusetts General Hospital and Harvard Medical School). This research was supported in part by National Institutes of Health Grants P50 CA086355 (to R.W. and M.J.P.), R24-CA92782 (to R.W.), and U54 CA126515–01 (to R.W.). M.J.P. was in part supported by the Human Frontier Science Program Organization (Grant LT00369/2003). C.R.B is supported by a fellowship from the Swiss National Science Foundation. P.R. is supported in part by a grant, Cancer Immunotherapy, from the European Community's sixth framework program.

1. Boon T, Coulie PG, Van den Eynde BJ, van der Bruggen P (2006) *Annu Rev Immunol* 24:175–208.
2. Zitvogel L, Tesniere A, Kroemer G (2006) *Nat Rev Immunol* 6:715–727.
3. Yee C, Greenberg P (2002) *Nat Rev Cancer* 2:409–419.
4. Dunn GP, Old LJ, Schreiber RD (2004) *Annu Rev Immunol* 22:329–360.
5. Romero P, Dunbar PR, Valmori D, Pittet M, Ogg GS, Rimoldi D, Chen JL, Lienard D, Cerottini JC, Cerundolo V (1998) *J Exp Med* 188:1641–1650.
6. Zippelius A, Batard P, Rubio-Godoy V, Bioley G, Lienard D, Lejeune F, Rimoldi D, Guillaume P, Meidenbauer N, Mackensen A, *et al.* (2004) *Cancer Res* 64:2865–2873.

7. Munn DH, Mellor AL (2006) *Immunol Rev* 213:146–158.
8. Ercolini AM, Ladle BH, Manning EA, Pfannenstiel LW, Armstrong TD, Machiels JP, Bieler JG, Emens LA, Reilly RT, Jaffee EM (2005) *J Exp Med.*
9. Sakaguchi S (2005) *Nat Immunol* 6:345–352.
10. Wang HY, Lee DA, Peng G, Guo Z, Li Y, Kiniwa Y, Shevach EM, Wang RF (2004) *Immunity* 20:107–118.
11. Chen ML, Pittet MJ, Gorelik L, Flavell RA, Weissleder R, von Boehmer H, Khazaie K (2005) *Proc Natl Acad Sci USA* 102:419–424.
12. Mempel TR, Pittet MJ, Khazaie K, Weninger W, Weissleder R, von Boehmer H, von Andrian UH (2006) *Immunity* 25:129–141.
13. Curiel TJ, Coukos G, Zou L, Alvarez X, Cheng P, Mottram P, Evdemon-Hogan M, Conejo-Garcia JR, Zhang L, Burow M, *et al.* (2004) *Nat Med* 10:942–949.
14. Sato E, Olson SH, Ahn J, Bundy B, Nishikawa H, Qian F, Jungbluth AA, Frosina D, Gnjatic S, Ambrosone C, *et al.* (2005) *Proc Natl Acad Sci USA* 102:18538–18543.
15. Gattinoni L, Powell DJJ, Rosenberg SA, Restifo NP (2006) *Nat Rev Immunol* 6:383–393.
16. June CH (2007) *J Clin Invest* 117:1466–1476.
17. Benlalam H, Vignard V, Khammari A, Bonnin A, Godet Y, Pandolfino MC, Jotereau F, Dreno B, Labarriere N (2007) *Cancer Immunol Immunother* 56:515–526.
18. Yee C, Thompson JA, Byrd D, Riddell SR, Roche P, Celis E, Greenberg PD (2002) *Proc Natl Acad Sci USA* 99:16168–16173.
19. Dudley ME, Wunderlich JR, Robbins PF, Yang JC, Hwu P, Schwartzentruber DJ, Topalian SL, Sherry R, Restifo NP, Hubicki AM, *et al.* (2002) *Science* 298:850–854.
20. Morgan RA, Dudley ME, Wunderlich JR, Hughes MS, Yang JC, Sherry RM, Royal RE, Topalian SL, Kammula US, Restifo NP, *et al.* (2006) *Science* 314:126–129.
21. Dudley ME, Wunderlich JR, Yang JC, Sherry RM, Topalian SL, Restifo NP, Royal RE, Kammula U, White DE, Mavroukakis SA, *et al.* (2005) *J Clin Oncol* 23:2346–2357.
22. Bulte JW, Douglas T, Witwer B, Zhang SC, Strable E, Lewis BK, Zywicke H, Miller B, van Gelderen P, Moskowitz BM, *et al.* (2001) *Nat Biotechnol* 19:1141–1147.
23. Koehne G, Doubrovin M, Doubrovina E, Zanzonico P, Gallardo HF, Ivanova A, Balatoni J, Teruya-Feldstein J, Heller G, May C, *et al.* (2003) *Nat Biotechnol* 21:405–413.
24. Weissleder R (2002) *Nat Rev Cancer* 2:11–18.
25. Negrin RS, Contag CH (2006) *Nat Rev Immunol* 6:484–490.
26. Murakami T, Cardones AR, Finkelstein SE, Restifo NP, Klaunberg BA, Nestle FO, Castillo SS, Dennis PA, Hwang ST (2003) *J Exp Med* 198:1337–1347.
27. Berger C, Flowers ME, Warren EH, Riddell SR (2006) *Blood* 107:2294–2302.
28. Kraitchman DL, Tatsumi M, Gilson WD, Ishimori T, Kedziorek D, Walczak P, Segars WP, Chen HH, Fritzges D, Izbudak I, *et al.* (2005) *Circulation* 112:1451–1461.
29. Swirski FK, Pittet MJ, Kircher MF, Aikawa E, Jaffer FA, Libby P, Weissleder R (2006) *Proc Natl Acad Sci USA* 103:10340–10345.
30. Boissonnas A, Fetler L, Zeelenberg IS, Hugues S, Amigorena S (2007) *J Exp Med* 204:345–356.
31. Mrass P, Takano H, Ng LG, Daxini S, Lasaro MO, Iparraguirre A, Cavanagh LL, von Andrian UH, Ertl HC, Haydon PG, Weninger W (2006) *J Exp Med* 203:2749–2761.
32. Rapoport AP, Stadtmauer EA, Aqui N, Badros A, Cotte J, Chrisley L, Veloso E, Zheng Z, Westphal S, Mair R, *et al.*(2005) *Nat Med* 11:1230–1237.
33. Dummer W, Niethammer AG, Baccala R, Lawson BR, Wagner N, Reisfeld RA, Theofilopoulos AN (2002) *J Clin Invest* 110:185–192.
34. Gattinoni L, Finkelstein SE, Klebanoff CA, Antony PA, Palmer DC, Spiess PJ, Hwang LN, Yu Z, Wrzesinski C, Heimann DM, *et al.* (2005) *J Exp Med* 202:907–912.
35. Wang LX, Shu S, Plautz GE (2005) *Cancer Res* 65:9547–9554.
36. Leen AM, Myers GD, Sili U, Huls MH, Weiss H, Leung KS, Carrum G, Krance RA, Chang CC, Molldrem JJ, *et al.* (2006) *Nat Med* 12:1160–1166.
37. Riddell SR, Bleakley M, Nishida T, Berger C, Warren EH (2006) *Biol Blood Marrow Transplant* 12:9–12.
38. Goulmy E (2006) *Hum Immunol* 67:433–438.
39. Battaglia M, Roncarolo MG (2006) *Inflamm Allergy Drug Targets* 5:157–165.
40. Battaglia M, Stabilini A, Draghici E, Migliavacca B, Gregori S, Bonifacio E, Roncarolo MG (2006) *Diabetes* 55:1571–1580.
41. Gattinoni L, Klebanoff CA, Palmer DC, Wrzesinski C, Kerstann K, Yu Z, Finkelstein SE, Theoret MR, Rosenberg SA, Restifo NP (2005) *J Clin Invest* 115:1616–1626.
42. Waldmann TA (2006) *Nat Rev Immunol* 6:595–601.
43. Zeng R, Spolski R, Finkelstein SE, Oh S, Kovanen PE, Hinrichs CS, Pise-Masison CA, Radonovich MF, Brady JN, Restifo NP, *et al.* (2005) *J Exp Med* 201:139–148.
44. Quezada SA, Peggs KS, Curran MA, Allison JP (2006) *J Clin Invest* 116:1935–1945.
45. Grimm J, Kirsch DG, Windsor SD, Kim CF, Santiago PM, Ntziachristos V, Jacks T, Weissleder R (2005) *Proc Natl Acad Sci USA* 102:14404–14409.
46. Ascher NL, Ahrenholz DH, Simmons RL, Weiblen B, Gomez L, Forstrom LA, Frick MP, Henke C, McCullough J (1979) *Arch Surg* 114:386–392.
47. Zhou R, Thomas DH, Qiao H, Bal HS, Choi SR, Alavi A, Ferrari VA, Kung HF, Acton PD (2005) *J Nucl Med* 46:816–822.
48. Hanson HL, Donermeyer DL, Ikeda H, White JM, Shankaran V, Old LJ, Shiku H, Schreiber RD, Allen PM (2000) *Immunity* 13:265–276.